PLANETARY SCIENCE

High-precision U-Pb zircon dating identifies a major magmatic event on the Moon at 4.338 Ga

Mélanie Barboni[1]*†, Dawid Szymanowski[2,3]*†, Blair Schoene[3], Nicolas Dauphas[4], Zhe J. Zhang[4], Xi Chen[4], Kevin D. McKeegan[5]

The Moon has had a complex history, with evidence of its primary crust formation obscured by later impacts. Existing U-Pb dates of >500 zircons from several locations on the lunar nearside reveal a pronounced age peak at 4.33 billion years (Ga), suggesting a major, potentially global magmatic event. However, the precision of existing geochronology is insufficient to determine whether this peak represents a brief event or a more protracted period of magmatism occurring over tens of millions of years. To improve the temporal resolution, we have analyzed Apollo 14, 15, and 17 zircons that were previously dated by ion microprobe at ~4.33 Ga using isotope dilution thermal ionization mass spectrometry. Concordant dates with sub-million-year uncertainty span ~4 million years from 4.338 to 4.334 Ga. Combined with Hf isotopic ratios and trace element concentrations, the data suggest zircon formation in a large impact melt sheet, possibly linked to the South Pole–Aitken basin.

INTRODUCTION

Analyses of samples retrieved by the Apollo missions (Fig. 1, A and B) have revealed that the Moon originated from a nearly fully molten state, with subsequent mineralogical and chemical differentiation during cooling and solidification of the lunar magma ocean (LMO) giving rise to a layered structure of the lunar crust and mantle (*1*). Subsequent magmatism and impacts have additionally left imprints on lunar rocks complicating efforts to discern the Moon's early history. For example, evidence for a spike in large basin-forming impacts ~4.0 to 3.8 billion years ago (Ga), suggesting a "terminal lunar cataclysm" (*2*), was initially proposed based on U-Pb analyses that indicated the presence of a parentless radiogenic Pb component widely distributed among nearside lunar rocks and soils. Later $^{40}Ar/^{39}Ar$ dating was interpreted as confirming a spike in impacts (*3*), but the Moon's early impact history is obscured in $^{40}Ar/^{39}Ar$ data due to saturation of the lunar surface from numerous impacts (*4*, *5*). In contrast, most applications of the Rb-Sr and Sm-Nd chronometers have focused on determining igneous ages rather than dating impact events (*6*, *7*).

Zircon crystals found in Apollo samples provide an alternative means to unravel the complex records of early lunar events through U-Pb dating, trace element concentrations, and Hf isotope compositions (*8*–*18*). To date, in situ secondary ion mass spectrometry (SIMS; or ion microprobe) analyses have determined over 500 Apollo and lunar meteorite zircon ages. Zircons from Apollo 14, 15, and 17 samples (and, to a lesser extent, from lunar meteorites) show a pronounced peak in $^{207}Pb/^{206}Pb$ ages at ~4.33 Ga (Fig. 1C). This peak may mark the final crystallization of the LMO (*19*, *20*) or it could reflect a spike in global magmatism triggered by a massive impact event such as the formation of the South Pole–Aitken (SPA) basin (*21*, *22*). Distinguishing between these scenarios is difficult because the precision of SIMS analyses is insufficient to determine whether zircon ages reflect a brief catastrophic melting event or more protracted magmatic processes spanning tens of millions of years (*16*). In this study, we selected Apollo 14, 15, and 17 zircon crystals that were previously dated by SIMS at around 4.33 Ga (*16*, *17*). We analyzed these crystals using a more precise methodology, isotope dilution thermal ionization mass spectrometry (ID-TIMS), to obtain new U-Pb dates. The ID-TIMS technique yields uncertainties as low as ~500 thousand years (2σ), enabling examination of both the precise timing and potential duration of zircon crystallization events at 4.33 Ga. Combined with trace element compositions and neutron capture-corrected initial Hf isotopic ratios of the dated zircons (*23*), we then use these data to discuss the timing and nature of events on the early Moon.

RESULTS

We targeted 13 zircon crystals with published in situ $^{207}Pb/^{206}Pb$ dates around 4.3 Ga collected across three Apollo sites (11 of which gave ages around 4.33 Ga): 10 from Apollo 14, one from Apollo 15, and two from Apollo 17 (Fig. 2). To isolate concordant age domains, the zircons underwent a stepwise dissolution procedure with two 6-hour, 180°C partial digestion steps in hydrofluoric acid (leachates 1 and 2, abbreviated L1 and L2) followed by complete 210°C acid digestion of the remaining residue (R) (*15*). All zircon residues yielded near-concordant ID-TIMS dates [within ~0.3% of the $^{207}Pb/^{235}U$-$^{206}Pb/^{238}U$ concordia curve defined by the mean values of the U decay constants (*24*); Fig. 2 and data S1]. Most $^{207}Pb/^{206}Pb$ dates also showed good agreement with the corresponding in situ SIMS results (fig. S2).

The first leachates (L1) had elevated common lead (Pb_c) and were often discordant (reflecting contamination) and so they were excluded from further interpretation. The second leachates (L2) and residues (R) displayed variable radiogenic Pb* to common Pb ratios (Pb^*/Pb_c = 9 to 2583), affecting sensitivity to the assumed Pb_c composition (fig. S3). Residue dates are most reliable, with Pb^*/Pb_c of 90 to 2583 making them highly insensitive to Pb_c corrections. Their concordance also suggests closed-system U-Pb behavior since zircon

[1]School of Earth and Space Exploration, Arizona State University, Tempe, AZ 85281, USA. [2]Institute of Geochemistry and Petrology, ETH Zurich, 8092 Zurich, Switzerland. [3]Department of Geosciences, Princeton University, Princeton, NJ 08544, USA. [4]Origins Laboratory, Department of the Geophysical Sciences and Enrico Fermi Institute, The University of Chicago, Chicago, IL 60637, USA. [5]Department of Earth, Planetary, and Space Sciences, University of California, Los Angeles, CA 90095, USA. *Corresponding author. Email: mbarboni@asu.edu (M.B.); dawid.szymanowski@erdw.ethz.ch (D.S.)
†These authors contributed equally to this work.

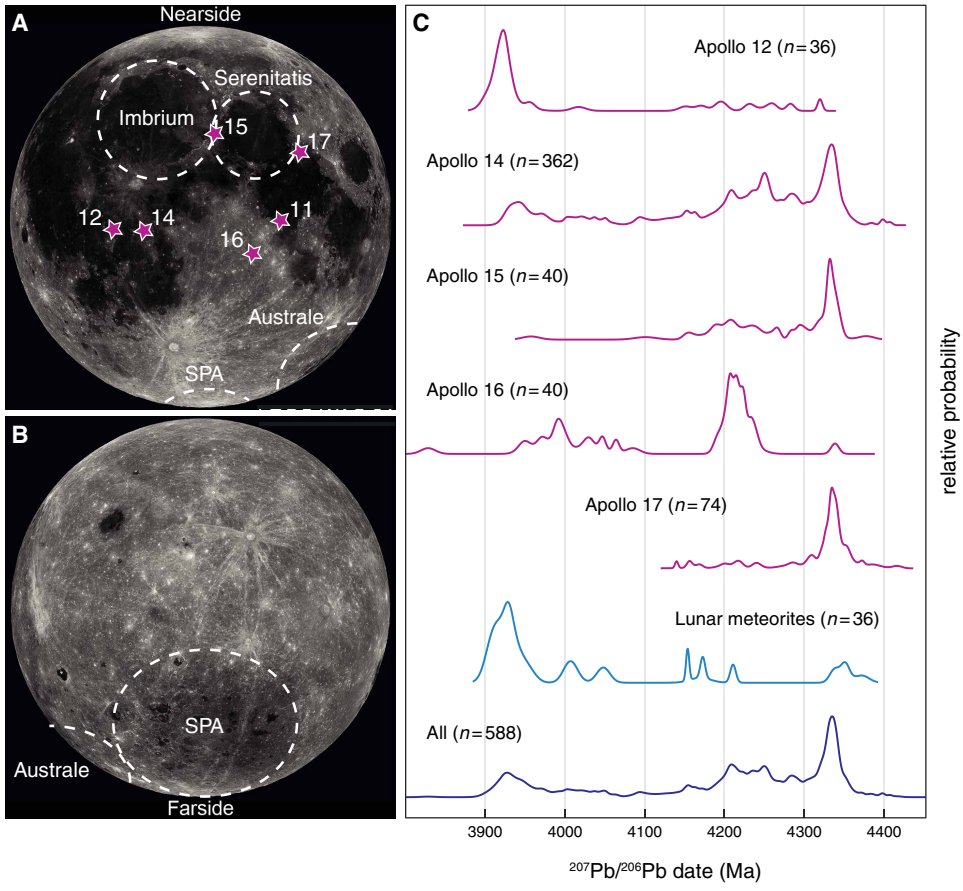

Fig. 1. Previous lunar zircon chronology. (**A** and **B**) Images of the near (A) and far (B) side of the Moon indicating the landing locations of Apollo missions and the major lunar basins. SPA, South Pole–Aitken. Images from NASA. (**C**) Distributions of previously reported SIMS $^{207}Pb/^{206}Pb$ dates obtained on zircons from Apollo samples and from lunar meteorites. A complete list of references is available in data S1.

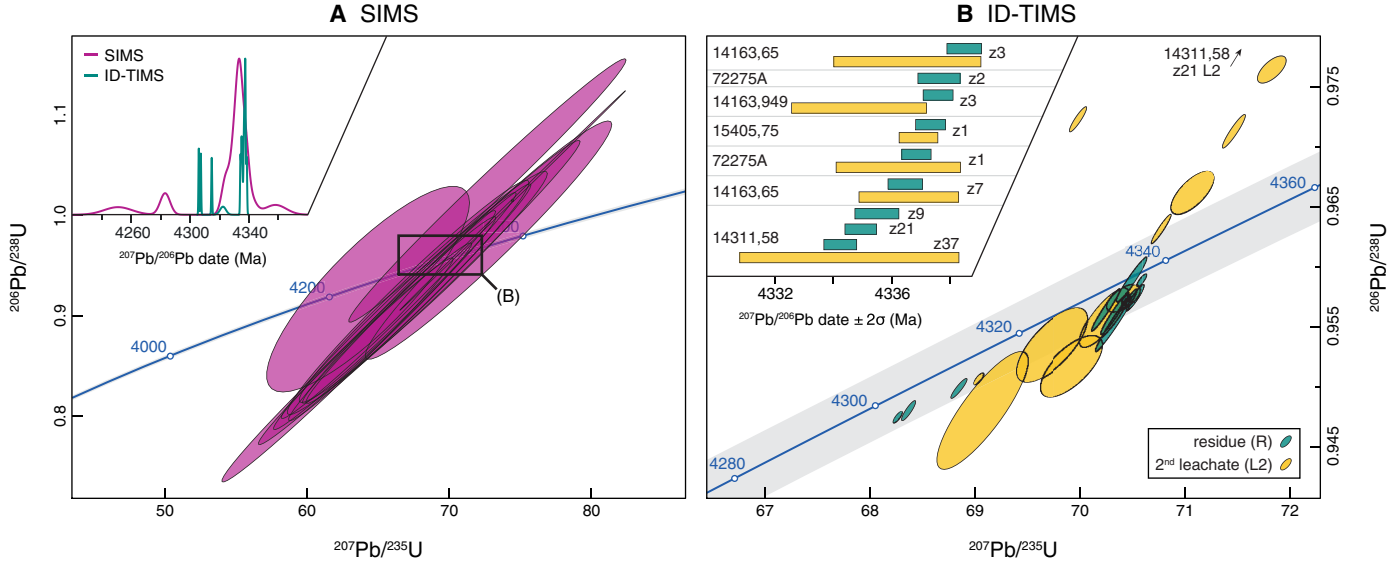

Fig. 2. New U-Pb dating of 4.3-Ga Apollo zircons. Wetherill concordia diagrams illustrating SIMS (**A**) and ID-TIMS (**B**) U-Pb dates for zircons in this study with their 95% confidence envelopes. ID-TIMS results, also shown as inset of rank-ordered $^{207}Pb/^{206}Pb$ dates within the main 4.33-Ga peak, are divided into residue (R) and second leachate (L2) aliquots. Samples with the prefix 14 are from Apollo 14; 15, Apollo 15; and 7, Apollo 17.

formation; thus, residues are the focus of our interpretations. In contrast, second leachates (L2) show variable levels of discordance including some analyses that are reversely discordant ($^{206}Pb/^{238}U$ date > $^{207}Pb/^{235}U$ date). Reverse discordance is caused by elemental fractionation of U from Pb; in this case, it appears to have occurred without Pb isotope fractionation, resulting in L2 $^{207}Pb/^{206}Pb$ dates that are in most cases consistent with those of the respective zircon residue. On the basis of acid leaching experiments (*25*), we suggest that the presence of this effect in some L2 leachates is an artifact resulting from partial dissolution rather than a natural feature.

Analytical repeatability of $^{207}Pb/^{206}Pb$ dates was determined to be better than 0.01% relative standard deviation through analysis of a synthetic 4.56-Ga U-Pb solution (data S1) (*26*). This confirms that analytical issues associated with mass spectrometry do not create additional scatter in our U-Pb isotope data. Accuracy and concordance of the U-Pb dates instead depend on:

1) The assumed origin and composition of the common Pb (Pb_c) component. While some L2 Pb_c exceeds expected laboratory contamination (data S1), sensitivity tests show that even assuming endmember lunar Pb_c compositions ranging from primordial [e.g., Canyon Diablo troilite (*27*)] to hypothetical highly radiogenic lunar Pb_c (*28*) would cause minimal change (< uncertainty) to the residue $^{207}Pb/^{206}Pb$ dates (fig. S3). Anomalous Pb_c compositions may further affect discordant L2 analyses but leave the radiogenic residues unchanged.

2) The assumed mass of laboratory blank U, which affects concordance but not $^{207}Pb/^{206}Pb$ dates (fig. S4).

3) The assumed zircon $^{238}U/^{235}U$ of 137.818 ± 0.045, consistent with terrestrial magmatic accessory minerals (*29*, *30*). Substantial deviations in lunar zircon outside this range [e.g., from cosmic ray–induced fission (*31*)] may cause additional uncertainty but this is difficult to quantify (fig. S4).

Applying the most conservative data reduction assumptions, we obtained 23 near-concordant L2 and R aliquots from 13 zircons (Fig. 2B and data S1). Eight aliquots gave $^{207}Pb/^{206}Pb$ dates between 4300 and 4330 million years (Ma), while most of the dates cluster around 4336 Ma. Considering only residues and high Pb^*/Pb_c L2s within that cluster, we observed a well-resolved range of $^{207}Pb/^{206}Pb$ dates from 4338.47 ± 0.59 Ma to 4334.24 ± 0.56 Ma. While this cluster is primarily defined by the Apollo 14 samples, the ages of the three Apollo 15 and 17 samples fall within it.

Following U-Pb dating, we analyzed the leachate and residue fractions of the zircons for trace element concentrations and Hf isotopic compositions (data S1). The zircon Hf isotopic ratios required correcting for neutron capture effects from cosmic ray exposure in lunar rocks (*23*, *32*, *33*). After applying this correction, all initial $\varepsilon^{176}Hf$ values for the 4338 to 4334-Ma zircons are indistinguishable at −1.13 ± 0.73 [2σ, SE on the weighted mean $\varepsilon^{176}Hf$ for the 4.33-Ga peak, chondrite uniform reservoir values from (*34*); Fig. 3A and data S1]. However, these zircons do display more heterogeneity in various elemental concentrations and ratios (Fig. 3, B and C, and data S1).

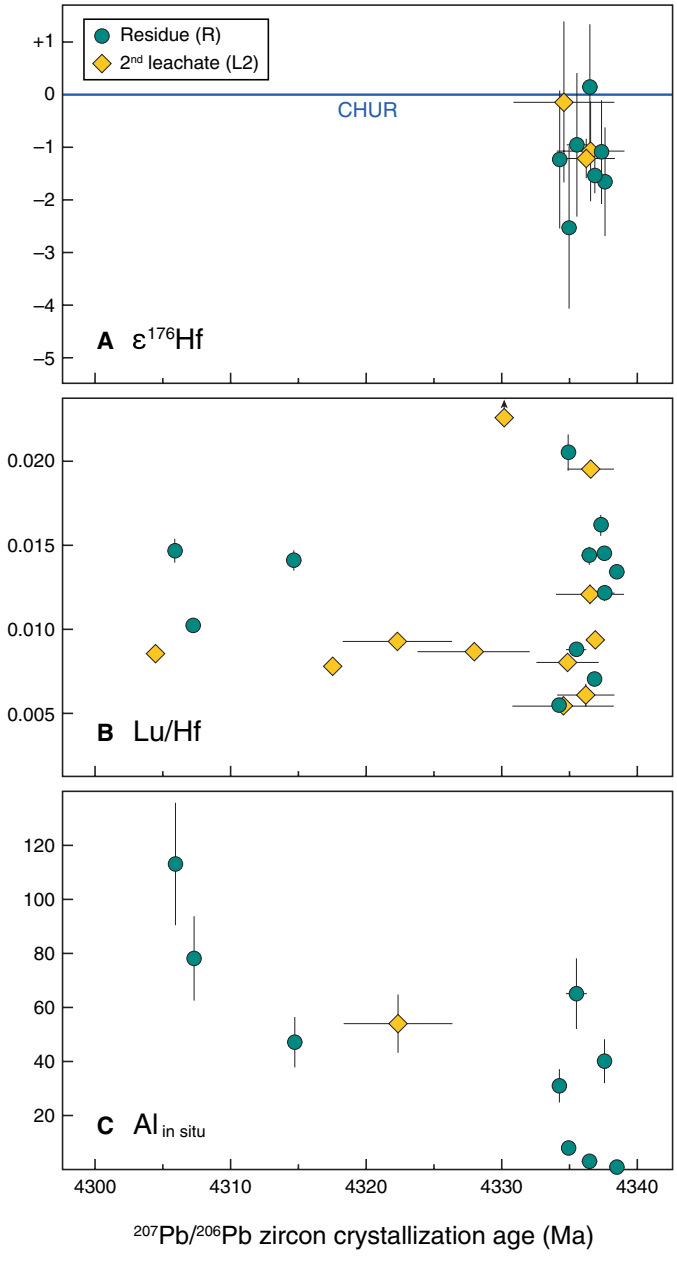

Fig. 3. Hafnium isotopes and trace elements in zircon. (**A**) Neutron capture corrected $\varepsilon^{176}Hf$ versus ID-TIMS age for the 4.33-Ga zircons presented in this study; (**B**) Lu/Hf versus age; (**C**) in situ Al (ppm) in zircon versus best ID-TIMS age. Al in zircon has been shown to be an indicator of the major element composition of the melt; for a given temperature, a melt with higher alumina activity (i.e., Al concentration) will produce zircons with higher Al than a low alumina activity melt (*17*, *90*).

DISCUSSION

Examining sampling biases

The peak of zircon crystallization ~4.33 Ga documented in several ion probe studies of lunar zircon has been interpreted to represent the occurrence of a global magmatic event(s) on the nearside of the Moon (*9*, *13*, *16*). To explore the nature and duration of this apparent zircon crystallization pulse, we analyzed 11 grains that were previously dated by SIMS at ~4.33 Ga, sourced from Apollo 14, 15, and 17 landing sites spanning hundreds of kilometers (Fig. 1A). By applying the more precise ID-TIMS method, we obtained new U-Pb dates on this subset. Eight of the 11 grains yielded ID-TIMS $^{207}Pb/^{206}Pb$ dates concentrated within a mere ~4 Ma span centered around 4336 Ma. While this subset represents just 5% of all ~4.33-Ga SIMS lunar zircon analyses reported to date (n = 186 grains), Monte Carlo simulations (n = 10,000 draws) indicate a <1% probability that a random

draw of 11 ~4330-Ma SIMS grains would produce a subset of 8 grains with ID-TIMS ages clustered between 4334 and 4338 Ma. Therefore, we can conclude with statistical confidence that the apparent ~4.33-Ga SIMS peak, for which uncertainties are on the order of tens of millions of years, has now been resolved by ID-TIMS to fall within a ~4 million-year window of zircon crystallization and that this is not due to a chance selection of grains that fortuitously fall within that narrow range. Additional zircon U-Pb dates between ~4305 and 4320 Ma were also found, which could potentially relate to similar lunar process(es) (impact or LMO differentiation). While expanding the high-precision ID-TIMS dataset is an important next step, our results reveal that the ~4.33-Ga zircon population is heterogeneous in its crystallization history over a 4-Ma time scale. We use the distinct subset of zircons dated to 4338 to 4334 Ma, combined with associated trace element and Hf isotopic signatures, to begin unravelling the origins of this apparent spike in zircon production on the early Moon.

Do the U-Pb dates represent zircon crystallization?

The U-Pb system in zircon is highly resistant to thermal disturbance (*35*); however, postcrystallization Pb loss remains a possibility for lunar grains that likely experienced impact shocks (*9*, *36*–*39*), potentially biasing the apparent duration of our 4.33-Ga peak. Identifying ancient (4 Ga or older) Pb loss in the zircons examined here is difficult since its trajectory in the U-Pb space would be essentially parallel to the concordia curve, resulting in little to no apparent discordance. Several studies investigating potential Pb loss in lunar zircons linked to impacts focused on within-grain SIMS $^{207}Pb/^{206}Pb$ age distributions and microtextures and concluded that the best criterion to identify zircons with reliable ages is intragrain consistency, in particular if ages agree within primary textural domains identified in cathodoluminescence (CL) (*37*, *40*). The studied zircons are all fragments of larger crystals that show uniform internal textures with no evidence that they contain more than a single zone (*17*) (fig. S1), suggesting a relatively simple crystallization history. Unfortunately, only one SIMS $^{207}Pb/^{206}Pb$ spot per grain was originally analyzed on these zircons (*16*, *17*), preventing us from assessing the intragrain age variability with in situ data. However, we find a good level of high-precision $^{207}Pb/^{206}Pb$ age consistency in R-L2 pairs within the 4.33-Ga peak (Fig. 2B), suggesting that if the zircons suffered partial Pb loss postdating their original crystallization, its timing was likely constrained to within the observed 4.33-Ga peak itself. While we cannot categorically exclude early partial Pb loss, complete Pb loss and resetting is unlikely, so its potential effect would be of increasing the apparent duration of the prominent 4.33-Ga age peak. Consequently, the true duration of zircon crystallization in the sampled magmatic event was at most ~4 million years.

Meaning of the 4.33-Ga peak

Considering the arguments developed above, we interpret our 4.33-Ga zircons to represent a major, potentially global magmatic event happening on the Moon at that time. We explore here three scenarios (summarized in Fig. 4) that could yield zircon crystallization in a narrow time window and explain finding these zircons throughout a large portion of the Moon's nearside. The first one is zircon crystallization in the KREEP residual melt that records final solidification of the LMO (*10*, *12*). The second scenario invokes a large impact, resulting in zircon formation in the differentiating melt sheet (*16*, *38*) and dissemination over the nearside of the Moon via subsequent impact events (*41*, *42*). The third option is a short period of intense impact activity where melt sheet zircons result from multiple impacts (*9*). Each hypothesized scenario would yield

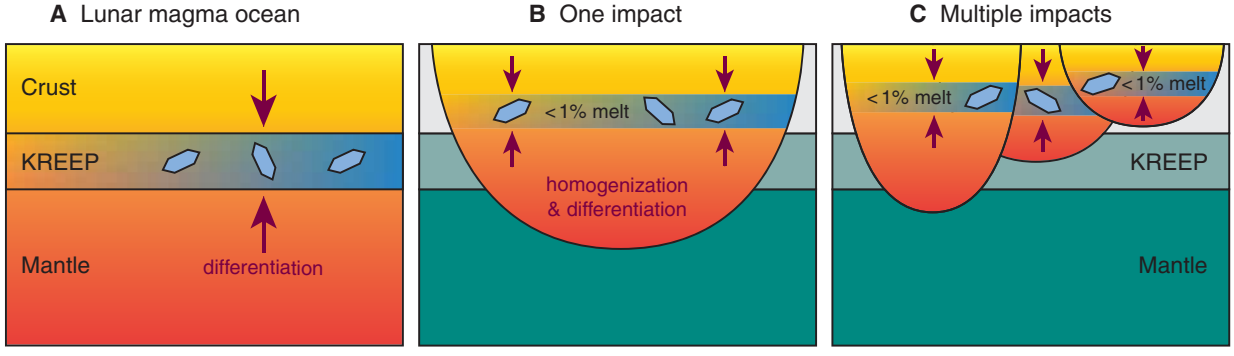

	A Lunar magma ocean	B One impact	C Multiple impacts
U–Pb ages	Wide age peak with onset at >4.46 Ga	**Narrow age peak** ✔	A range of ages
Hf isotopes	Temporal variations reflecting evolution of KREEP	**Homogeneous isotopic ratios** ✔	Heterogeneous isotopic ratios
trace elements	**Heterogeneous, reflecting local crystallization conditions in the last pockets of melt** ✔		

Fig. 4. Three possible scenarios to form the observed peak in zircon crystallization age at 4.338 Ga. (**A**) Formation in the final melts of the LMO, (**B**) formation in a large, homogenized impact melt sheet, and (**C**) formation within multiple impact melt sheets formed around 4.338 Ga. Table indicates if the observed age distribution, Hf isotope, and trace element compositions meet what is expected for each scenario (see text for details).

different distributions of U-Pb ages, as well as Hf isotope and trace element characteristics that we consider below.

The possibility of the 4.33-Ga zircon population originating from late-stage LMO (Fig. 4A) crystallization is considered first since the KREEP reservoir must have supplied Zr for primary zircon growth (*10*, *38*) and LMO solidification would be a global process that could produce primordial lunar zircons across widespread Apollo sites (*1*). The apparent preponderance of ages around 4.3 Ga recorded in diverse lunar samples dated by different radiometric systems (^{207}Pb-^{206}Pb, ^{147}Sm-^{143}Nd, and ^{146}Sm-^{142}Nd) has been used to suggest that the Moon itself formed around that time, although a global secondary magmatic event such as a large impact was not excluded [see discussion in (*19*) and (*20*)]. However, Moon formation around 4.3 Ga is in contradiction with ages of the oldest lunar zircons found in multiple Apollo samples (Fig. 5) and reported at 4460 ± 31 Ma (sample 72255), 4416 ± 35 Ma (14304), 4404 ± 20 Ma (14321), 4429 ± 55 Ma (15405), 4409 ± 13 Ma (73235), and 4417 ± 6 Ma (72215) [all concordant analyses, errors reported as 1σ (*9*, *10*, *12*, *13*, *18*, *36*, *39*); Fig. 5]. In principle, a disturbance of the typically robust zircon U-Pb system could possibly compromise these old ages; however, a recent study (*18*) using atom probe tomography demonstrated that the oldest grain documented until now (at 4460 Ma) shows no Pb clustering, supporting the ability of this old age to record primary lunar crystallization rather than later impact mobilization. Additional reliability indicators come from the age consistency between grain fragments and lack of complex zoning in several of these >4.4-Ga zircons (*10*, *12*, *13*). Melt evolution modeling constrains the start of zircon crystallization to when the LMO exceeds 99.9% solidification (*43*). Hence, the oldest zircons likely date near-final LMO lockup, no later than ~4430 Ma. A near-complete LMO solidification by ~4430 Ma is corroborated by 4.41- to 4.47-Ga Lu-Hf model ages measured for the KREEP reservoir [whole-rock and zircon data (*32*)], assumed to represent the last LMO residual melt, and zircon Hf isotopic evidence suggesting separation of urKREEP from the LMO by no later than ~4.5 Ga (*15*). For the observed 4.33-Ga lunar zircon population to have crystallized from residual LMO melts would require that fractionated, low-volume melts persisted for a protracted period of at least ~90 million years after initial LMO solidification (Fig. 5). Estimates of LMO life span derived from thermal modeling show a range of results, with some models permissive of the LMO existing until our zircon peak and others prohibiting it (fig. S5) (*44*–*50*). While several LMO thermal models indicate solidification extending beyond 4.33 Ga, such slowly cooled LMO should produce zircons with a wide distribution of crystallization age rather than a distribution centered on one narrow peak at 4.33 Ga. The conspicuous scarcity of zircon ages between 4.43 and 4.33 Ga followed by a marked peak at 4336 ± 2 Ma (Fig. 5) is thus inconsistent with an age distribution expected from slowly cooling residual LMO melts. We conclude that the pronounced peak at 4.33 Ga more likely reflects rapid zircon production in an episodic event. Our preferred explanation is the occurrence of a very large impact, leading to new, concordant zircons crystallizing in the differentiating melt sheet that had incorporated a KREEP component (*14*, *38*). Such an impact event would also align with finding ca. 4.33-Ga zircons across multiple Apollo sites, as gardening by subsequent cratering would disseminate material over a wide area (*41*, *42*). Last, we note that such a large impact could disturb whole-rock isochron ages potentially explaining some of the 4.3 Ga ages recorded by the ^{207}Pb-^{206}Pb, ^{147}Sm-^{143}Nd, and ^{146}Sm-^{142}Nd systems in multiple lunar samples (*19*, *20*).

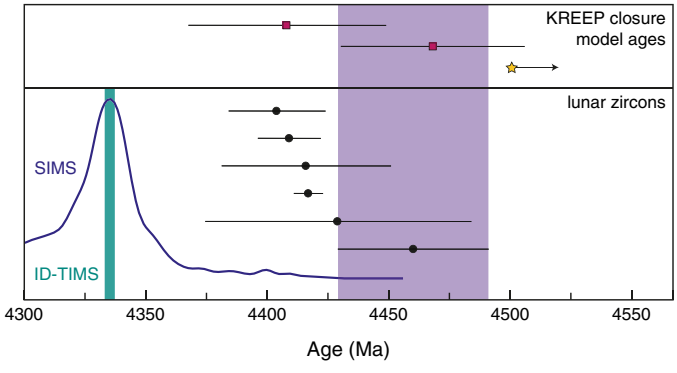

Fig. 5. Zircon data relevant to the timing of LMO solidification. Oldest Apollo zircon [4460 ± 31 Ma, sample 72255 (*18*, *39*), purple field] sets a minimum age of zircon saturation in KREEP (LMO > 99% crystallized). Also indicated: all published >4.4-Ga lunar zircon ^{207}Pb/^{206}Pb ages (*9*, *10*, *12*, *13*, *36*) (black, all concordant analyses), a distribution of all previously reported SIMS zircon ^{207}Pb/^{206}Pb dates >4.3 Ga (as in Fig. 1), minimum lunar crust-mantle differentiation time (*15*) (yellow star), KREEP model age obtained from Lu-Hf data on zircon and KREEP-rich samples (*32*), and our 4.33-Ga ID-TIMS peak.

As previously noted, it is conceivable that several smaller impacts occurring close to 4.33 Ga could also explain the zircon ages and wide distribution over the lunar surface (Fig. 4C). However, considering the homogeneity of Hf isotopic ratios in our 4.33-Ga grains (Fig. 3A), we suggest that zircon production from one large impact is more likely than from multiple, smaller impacts occurring within about 4 million years. Hafnium isotopic ratios across different lunar whole rocks show a large difference between mantle-derived samples [positive ε^{176}Hf up to +20 at 3.9 Ga (*32*)] and samples derived from the differentiated KREEP layer characterized by relatively unradiogenic ε^{176}Hf [−5.5 at 3.9 Ga (*32*)], although the total range of lunar ε^{176}Hf was necessarily smaller at 4.33 Ga. We hypothesize that in a multiple impact scenario, each impact would crystallize new zircons from a distinct melt sheet. These would likely have variable mixing proportions between crust, mantle, and KREEP components, generating more scattered Hf isotope ratios. To produce the tightly clustered Hf isotope ratios observed in our 4.33 Ga grains with multiple impacts would require a fortuitous consistency in target rock compositions (proportions of involved mantle, KREEP, and crust) occurring across multiple impact sites. In contrast, a single large impact could create a more extensive melt sheet allowing easier homogenization of distinct isotopic components (*51*). Thus, considering the compositional arguments, we favor the hypothesis of one large impact.

The peak in the zircon age distribution documented here lies within the ca. 30-Ma range (4364 to 4331 Ma) corresponding to a preponderance of ages for magnesium-suite (Mg-suite) rocks [see discussion in (*20*)]. The geochemical characteristics of the 4.33-Ga zircons, including the low Al content [<40 parts per million (ppm), apart from one analysis] suggesting limited involvement of ferroan anorthosite in their parental magmas (*17*) and enriched initial ε^{176}Hf values (−1.13 ± 0.73), are also reminiscent of the Mg-suite rocks. Mg-suite magmatism may reflect melting of a hybridized source comprising ultramafic cumulates, anorthosite crust, and KREEP, which could have been juxtaposed during mantle overturn. In this scenario, higher-density Fe-Ti oxides would sink, while lower-density olivine and pyroxene cumulates would rise. Although the broad

coincidence in age and geochemical characteristics between Mg-suite rocks and the peak in the zircon age distribution does not necessarily imply a genetic relationship, as zircons most likely crystallized from a purer KREEP component, a common genetic event such as a large impact could have triggered both the melting of the urKREEP layer and the destabilization of cumulates with contrasting densities.

A 4.338 Ga age for the SPA basin impact?

A large impact would have generated an extensive melt sheet (*41*) that evolved via fractional crystallization during cooling. As with LMO solidification, zircon saturation would be reached in the last stages, when the residual melt achieved appropriate Zr and SiO_2 concentrations (*43, 52*). Investigating the potential geometry and thermal evolution of such an impact melt sheet is difficult. While the Moon preserves abundant evidence of impacts, inferences about melt chemistry or evolution must rely on lunar breccia fragments with uncertain origins. We therefore consider an accessible analog: Earth's large impacts containing zircon that crystallized within the impact melt sheet (*53*). The ca. 1.8-Ga Sudbury impact (Canada) has been extensively studied and proposed as the best terrestrial proxy for large lunar basins, with demonstrated neoblastic zircon (*54*–*57*). The Sudbury complex is a layered igneous formation, interpreted as reflecting fractional crystallization of an originally homogeneous impact melt sheet and showing increasingly evolved lithologies upward through the structure (*54*–*56*). The impact occurred into a heterogeneous mixture of metasedimentary, metaigneous, and igneous target rocks with diverse mineralogy and geochemistry (*55*) and illustrates that large impact melt sheets have the potential to chemically homogenize and then differentiate. The Sudbury melt sheet appears to have quickly homogenized after formation, preserving apparently uniform Hf isotopic compositions throughout differentiation (*55*). Our 4.33-Ga lunar zircons show such homogeneous Hf, compatible with formation in a similarly large and well-mixed impact melt sheet. We note however that while capable of isotopic homogenization, these impact melt differentiation processes can also generate a spectrum of incompatible trace element compositions. This is reflected in Sudbury zircons, where (i) progressively differentiated layers contain zircons enriched in U, Th and REEs, and (ii) the most evolved zircons show the greatest trace element variability. This suggests late-stage melt heterogeneity and isolated melt pocket evolution (*56*). Given that lunar zircons would similarly crystallize from the last residual melt fractions, variable incompatible element abundances would be expected. Notably, our 4.33-Ga grains show divergence in Lu/Hf, Al and other indicators (Fig. 3, B and C, and data S1). In summary, while additional terrestrial impact research could better inform lunar comparisons, current observations seem consistent with a hypothesized 4.33-Ga impact melt origin, capable of (i) initial Hf isotopic homogenization and (ii) fractional crystallization allowing zircon saturation over a limited time interval (<5 million years).

Linking a potential large 4.338-Ga impact to a specific >4-Ga lunar basin is challenging, as early lunar chronology remains highly debated. Pre-Imbrium basin formation chronology relies on limited radiometric ages and stratigraphic/crater density constraints (*58*, *59*). Twenty-nine basins with apparent ages >4 Ga have been identified on the Moon, including the large SPA, Serenitatis, and Australe basins [(*60*, *61*); Fig. 1]. To explain the observed 4.33-Ga zircon peak, the impact should have: (i) produced a large and well-mixed melt sheet capable of homogenizing Hf isotope values, (ii) enabled melt differentiation and zircon saturation, and (iii) covered a large enough area to have fed samples to multiple Apollo landing sites through later cratering and ejecta transport. We set the age of this potential impact at 4.338 Ga, corresponding to the maximum of the range shown by our U-Pb data, because if the zircon-forming process was due to an impact, then the minimum impact age must be given by the oldest date, with the younger samples representing the cooling timescale. Although the precise source crater is currently unconstrained, the SPA basin, the oldest and largest recognized lunar basin, is a compelling candidate. SPA deeply excavated the crust and mantle (*62*, *63*), likely generating a huge impact melt sheet (*64*) that probably differentiated (*65*–*67*) and allowed zircon crystallization. SPA material has also been proposed as a source for Apollo 17 samples (*42*), suggesting that ejecta from later impacts into the SPA basin could potentially be disseminated over the nearside of the Moon. Future investigations into the potential petrogenetic relationships between the 4.338-Ga zircons and the SPA basin impact melt sheet could provide valuable insights into the early evolution of the Moon and the role of large impacts in shaping its crust.

Overall, our zircon results require a major lunar magmatic event at ~4.338 Ga. The age, short timespan for zircon crystallization, and geochemical and Hf isotopic characteristics of the zircons are most consistent with origin in a large, differentiating impact melt. New samples acquired from the lunar south pole by future sample return missions will help evaluate hypothesized links between this early magmatism and SPA itself.

MATERIALS AND METHODS

Samples

14311 (Apollo 14 site)

14311 is a coherent, polymict impact melt breccia with a cosmic ray exposure age estimated between 500 and 700 Ma (*68*). We have little information about what the zircon derived from the breccia sample looked like before crushing, as we did not have a thin section of this specific split of 14311. However, others have described this sample in detail identifying crystalline matrix breccia that is ~75% plagioclase (14311,94) (*69*). Plagioclase, gabbronorite, and granulitic clasts, as well as an ilmenite-filled cavity with a zircon, have also been documented (*36*, *69*). Clasts in this sample were interpreted to originate from the subregolith basement defined as the Fra Mauro Formation (*69*). Previous U-Pb zircon ages from 14311 show at least three distinct zircon age populations at 4334 ± 10 Ma, 4245 ± 10 Ma, and 3953 ± 10 Ma (*11*, *17*, *70*). CL imaging and details of the zircons used in this study are available in Trail *et al.* (*17*). All zircons are fragments ranging 100 to 500 μm in size and showing little CL response with some grains having slight oscillatory zoning.

14163 (Apollo 14 site)

Sample 14163 is a sub-mature soil characterized by a high KREEP component and high percentage of glass. Upon sieving, it was found to be largely free of rock fragments. The sample was determined to be >50% glass, including annealed breccias from the Fra Mauro formation (*71*). Mare-derived material is present, but likely only represents about 5% of the total material sampled (*71*). A small percentage of the glass was also classified as "granitic" (*71*), and approximately 15% of the glass fragments (*72*) yielded SiO_2 contents between 60 and 80 wt %. CL imaging and details of the zircons used in this study are available in Trail *et al.* (*17*). All zircons are fragments ranging

100 to 300 μm in size and showing little CL response and no obvious oscillatory zoning.

15405 (Apollo 15 site)

This sample is a clast-bearing impact-melt breccia presenting a crystalline matrix composed of fine-grained intergrown pyroxene, plagioclase, and ilmenite. Clasts include mineral fragments of plagioclase and pyroxene, along with lithic clasts of KREEP basalt, granite, and quartz monzodiorite. The zircon used in this study was described in Crow *et al.* (*16*). No CL imaging is available.

72275 (Apollo 17 site)

Sample 72275 is a feldspathic breccia, potentially ejecta from the Serenitatis basin (*73*), displaying a high abundance of KREEP-like non-mare basalt (*74*). Shih *et al.* (*75*) reported Rb-Sr and Sm-Nd ages for a KREEP basalt clast of 4.31 ± 0.08 and 4.08 ± 0.07 Ga, respectively. Zircons have previously been reported in 72275 and have ^{207}Pb-^{206}Pb ages ranging from 4.24 to 4.42 Ga (*12*, *13*). Eleven analyses of eight zircons by Crow *et al.* (*16*) yield weighted mean ^{207}Pb-^{206}Pb ages = 4334.3 ± 2.2 Ma (2σ). The zircons from the sample used in this study were described in Crow *et al.* (*16*). No CL imaging is available.

U-Pb zircon geochronology by SIMS

U-Th-Pb dating was performed on the UCLA CAMECA ims1290 using the Hyperion-II ion source for the primary beam. Details on the analytical procedure and data reduction can be found in Trail *et al.* (*17*).

In situ zircon trace element compositions by SIMS

Trace elements (including REE, Th, U, and Al) were measured with the UCLA CAMECA ims1290. Details on the analytical procedure and data reduction can be found in Trail *et al.* (*17*).

U-Pb zircon geochronology by ID-TIMS

Zircon crystals were analyzed for Pb and U isotope ratios by chemical abrasion–ID-TIMS at Princeton University. The selected crystals were first liberated from ion probe epoxy mounts and individually annealed for 48 hours in a 900°C muffle furnace. Following extensive rinsing in HCl and HNO_3, the crystals were subjected to a partial dissolution procedure [similar to (*76*)] consisting of two steps of leaching in ~90 μl of 29 M HF in individual 200-μl perfluoroalkoxy alkane (PFA) microcapsules assembled inside a Parr pressure vessel held for 6 hours in a 180°C oven. After each of the two partial dissolution steps (called L1 and L2), the HF leachate was pipetted off and kept for subsequent analyses, while the zircon residue was rinsed with HCl and HNO_3 and returned to the oven with 29 M HF for the next dissolution step. The complete dissolution step of the zircon residue (R) was achieved over 60 hours at 210°C. L1 and L2 solutions were spiked with one of the EARTHTIME (^{202}Pb-)^{205}Pb-^{233}U-^{235}U tracers (*77*, *78*) (ET535 for L1 and ET2535 for L2) and equilibrated on a hotplate, dried down, and redissolved in 6 M HCl. Zircon residues were spiked with ET2535 inside the 200-μl PFA microcapsules before final dissolution; the solutions were dried down and redissolved in 6 M HCl inside a Parr bomb (180°C for 12 hours) to convert to chloride form. All samples were dried and taken up in 3 M HCl in preparation for ion exchange chromatography separating U and Pb in microcolumns filled with 50 μl of AG1-X8 anion resin, following methods modified from Krogh (*79*). Each combined U-Pb fraction was dried down with a drop of 0.05 M H_3PO_4 and loaded in a microdrop of silica gel emitter (*80*) onto a single, outgassed, zone-refined Re filament for TIMS analysis.

Isotopic measurements were performed at Princeton University with a new Isotopx Phoenix TIMS equipped with ATONA amplifiers (*81*). Most samples were analyzed following the methods described by Szymanowski and Schoene (*81*), i.e., using a two-step FaraDaly method collecting $^{(202),\ 205\text{-}208}$Pb in Faraday cups and ^{204}Pb in the axial Daly/photomultiplier ion counting system (30-s integration), followed by a 10-s step analyzing ^{205}Pb in the Daly to correct for Faraday/Daly gain. Baselines for the ATONA-Faradays were acquired offline ("electronic baseline") over 12 h before analyses. Low Pb intensity samples (<ca. 1 mV on mass 206) were measured using peak-hopping mode on the Daly/photomultiplier. Potential interferences from $BaPO_2$ and Tl on masses 202, 204, and 205 were generally negligible over the duration of the project and were only monitored in some Daly analyses. Instrumental mass fractionation for Pb was corrected in-run using the measured ^{202}Pb/^{205}Pb of the ET2535 spike, or, for ET535-spiked samples, with a linear factor derived from a long-term compilation of ^{202}Pb/^{205}Pb values measured in spiked unknowns on the detector setup used [0.09 ± 0.04%/amu (2σ) for Faradays and 0.14 ± 0.07%/amu (2σ) for Daly]. The dead time of the Daly system was kept constant throughout the period of the study but was monitored with analyses of NIST SRM 982 Pb isotopic standard over a range of intensities. U isotope ratios were measured as UO_2 in static mode using 30-s integrations and corrected for mass fractionation using the ^{233}U/^{235}U of the spike, assuming a sample ^{238}U/^{235}U of 137.818 ± 0.045 (*29*). Whenever permitted by intensity, interferences in UO_2 analyses were corrected in-run using ^{18}O/^{16}O calculated using intensity on mass 269 (*81*), or else using an ^{18}O/^{16}O value of 0.00205 ± 0.00004 (2σ). All data reduction was accomplished with the Tripoli and ET_Redux software packages (*82*) using the algorithms of McLean *et al.* (*83*). U decay constants are from Jaffey *et al.* (*84*). A correction for secular disequilibrium in the ^{238}U-^{206}Pb system due to the exclusion of Th during zircon crystallization (*85*) was made for each analysis using a fixed Th/U_{melt} of 3.5 ± 2 (2σ) representative of average terrestrial magma (*86*). Changing Th/U_{melt} has a negligible effect on the ^{207}Pb/^{206}Pb dates. The amount of U blank was set at 0.02 ± 0.02 (2σ) pg based on total procedural blank measurements. This assumption may have an effect on the concordance of some low-U samples; however, it does not affect the accuracy of ^{207}Pb/^{206}Pb dates used for our interpretations (fig. S4).

The amount of common Pb (Pb_c) in the samples, calculated from the measured amount of ^{204}Pb, varied widely between elevated values in first leachates (L1) and values mostly in line with the amount of Pb_c expected from laboratory contamination (R). Elevated Pb_c in L1s is interpreted as a combination of removal of any surface contamination remaining from sample preparation as well as from dissolution of any mineral or melt inclusions. The preferential removal of inclusions, as well as the utilization of cracks or fractures as efficient dissolution pathways preferentially in the first leaching step, was recently shown with textural observations on partially leached zircons using a similar experimental setup (*87*). In contrast to L1s, residues only contained Pb_c in amounts consistent with those measured in total procedural blanks and in routine zircon runs at Princeton (0.08 to 0.36 pg), suggesting that (i) most inclusions and contamination had been removed in steps L1-L2 and (ii) all Pb_c in those samples was laboratory derived. Pb_c in L2s was generally more elevated than in residues (0.25 to 4.93 pg), which reflects their preparation including a pipetting step and larger volumes of reagents. While the relative masses of Pb_c in the three groups of samples are well

explained by various sources of terrestrial contamination, it is also conceivable that L1s and, less likely, L2s contained some amount of old lunar common Pb. The magnitude of this potential lunar contribution is difficult to constrain and correct for but it would have an effect on the accuracy of L1 and L2 dates (fig. S3). In summary, we consider it a valid assumption to correct all data with a terrestrial Pb_c composition but recognize a potential limitation to the accuracy of L1 and, to a lesser extent, L2 dates. The composition used was compiled from total procedural blanks prepared at Princeton University over a multiyear period: $^{206}Pb/^{204}Pb = 18.58 \pm 0.56$, $^{207}Pb/^{204}Pb = 15.87 \pm 0.67$, and $^{208}Pb/^{204}Pb = 38.18 \pm 1.23$ (all 2σ).

The viability of the sample preparation, mass spectrometry, and data reduction methods is supported by the repeatability of the synthetic solution ET 4567-R, the most radiogenic of a series of U-Pb solutions approximating the age of the solar system (*26*) (all data presented in data S1). Eight aliquots initially presented in Szymanowski and Schoene (*81*) were supplemented by another 12 aliquots of 50- to 850-pg Pb* ran over the course of the lunar zircon analyses with both the FaraDaly and Daly method for Pb, and reduced with one set of U isotopic ratios analyzed as for zircon unknowns. The weighted mean $^{207}Pb/^{206}Pb$ age was 4559.71 ± 0.14 Ma ($n = 36$, MSWD = 0.7). The accuracy of this result is currently difficult to evaluate due to the lack of absolute reference for the solution; however, the data demonstrate the excellent repeatability of our analytical approach in this age range.

Zircon trace element compositions (TIMS-TEA)

The trace element analyses (TEA) (*88*) were performed at Princeton University with methods similar to those applied in O'Connor *et al.* (*89*), reproduced here with minimal adjustments. All results are available in data S1.

Following the separation of U and Pb from individual zircons, wash fractions containing all constituent elements other than U and Pb were dried down and stored in polypropylene vials as chloride salts. The salts were then redissolved in 1 ml of 0.5 M HNO_3 + 0.015 M HF + 1 ppb In. Measurements of the solutions were performed on a Thermo iCAP quadrupole inductively coupled plasma mass spectrometer (ICP-MS) with a sample introduction system consisting of a PFA cyclonic spray chamber, a nebulizer with a nominal uptake rate of 100 μl/min, and an Elemental Scientific SC-μ DX autosampler. Sample uptake and analysis time added up to 3 min, consuming about 0.3 ml of the 1-ml sample solution. Measured elements included Zr, Hf, Y, Nb, Ta, REEs, Th, and In, where indium was used as internal standard during mass spectrometry. A matrix-matched, gravimetric external calibration solution was prepared with the relative abundance of targeted elements representing that observed in natural zircon (e.g., Zr/Hf = 50). A dilution series was generated using this solution to cover the range of concentrations observed in unknowns (e.g., [Zr] = 10 to 10^4 ng/g), which was then used to generate a concentration-intensity calibration curve for each element for every block of unknowns. Samples, reference solutions, and total procedural blanks were analyzed in blocks of 30 to 40. Following data acquisition, solution concentrations were converted to stoichiometric concentrations in zircon by normalizing solution concentration data assuming that all trace elements partition into the Zr^{4+} site in $ZrSiO_4$, where $\sum (Zr + Hf + ... + Th) = 497{,}646$ ppm. Uranium concentrations were not directly measured since U was included in the U-Pb aliquot used for ID-TIMS geochronology; instead, we reconstructed the zircon U content by combining the atomic Th/U estimated from ID-TIMS analyses with the Th concentration measured by ICP-MS. U and Th contents were then corrected for prior decay using the $^{207}Pb/^{206}Pb$ date of the aliquot to yield initial concentrations in zircon. Uncertainties in TE contents are reported at the 95% confidence level and include subtraction of the mean and SD of total procedural blank measurements. The typical repeatability of element ratios using the TEA method (1 SD) was 2% for Zr/Hf and 5 to 7% for most MREE-HREE ratios of interest [see O'Connor *et al.* (*89*) for an extended set of secondary reference solution analyses]. Because of its importance for ingrowth corrections of Hf-isotopic ratios, Lu/Hf ratio repeatability was additionally monitored using a set of two MUNZirc standard solutions (data S1).

Zircon Hf isotopic ratios

The aliquots remaining after U-Pb separation and TEA analyses were analyzed for Lu-Hf isotopes at the University of Chicago following the methodology detailed in Chen *et al.* (*23*). Hf isotopic ratios were corrected for neutron capture using two different approaches [using either the $\varepsilon^{176}Hf$-$\varepsilon^{178}Hf$ or the $\varepsilon^{176}Hf$-$\varepsilon^{180}Hf$ method (*23*)] and are presented in data S1. Because the stepwise chemical abrasion procedure used for U-Pb dating could have fractionated the Lu/Hf ratio by incongruent dissolution (potentially leading to inaccurate radiogenic ingrowth correction), we compared the calculated initial $\varepsilon^{176}Hf$ values from successive leaching steps and residues and based our interpretations only on residues and those L2s whose initial $\varepsilon^{176}Hf$ agreed with that of the respective residue (Fig. 3A).

Supplementary Materials

The PDF file includes:

Figs. S1 to S5

Legend for data S1

Other Supplementary Material for this manuscript includes the following:

Data S1

REFERENCES AND NOTES

1. J. A. Wood, J. S. Dickey Jr, U. B. Marvin, B. N. Powell, Lunar anorthosites and a geophysical model of the moon. *Proc. Lunar Sci. Conf.* **1**, 965–988 (1970).
2. F. Tera, D. A. Papanastassiou, G. J. Wasserburg, Isotopic evidence for a terminal lunar cataclysm. *Earth Planet. Sci. Lett.* **22**, 1–21 (1974).
3. G. Turner, P. H. Cadogan, C. J. Yonge, Argon selenochronology. *Proc. Lunar Sci. Conf.* **4**, 1889–1914 (1973).
4. W. K. Hartmann, Lunar "cataclysm": A misconception? *Icarus* **24**, 181–187 (1975).
5. P. Boehnke, T. M. Harrison, Illusory late heavy bombardments. *Proc. Natl. Acad. Sci. U.S.A.* **113**, 10802–10806 (2016).
6. L. E. Borg, J. N. Connelly, M. Boyet, R. W. Carlson, Chronological evidence that the Moon is either young or did not have a global magma ocean. *Nature* **477**, 70–72 (2011).
7. R. W. Carlson, L. E. Borg, A. M. Gaffney, M. Boyet, Rb-Sr, Sm-Nd and Lu-Hf isotope systematics of the lunar Mg-suite: The age of the lunar crust and its relation to the time of Moon formation. *Philos. Trans. R. Soc. A* **372**, 20130246 (2014).
8. M. L. Grange, A. A. Nemchin, R. T. Pidgeon, The effect of 1.9 and 1.4 Ga impact events on 4.3 Ga zircon and phosphate from an Apollo 15 melt breccia. *J. Geophys. Res. Planets* **118**, 2180–2197 (2013).
9. M. L. Grange, A. A. Nemchin, N. Timms, R. T. Pidgeon, C. Meyer, Complex magmatic and impact history prior to 4.1 Ga recorded in zircon from Apollo 17 South Massif aphanitic breccia 73235. *Geochim. Cosmochim. Acta* **75**, 2213–2232 (2011).
10. D. J. Taylor, K. D. McKeegan, T. M. Harrison, Lu–Hf zircon evidence for rapid lunar differentiation. *Earth Planet. Sci. Lett.* **279**, 157–164 (2009).
11. M. D. Hopkins, S. J. Mojzsis, A protracted timeline for lunar bombardment from mineral chemistry, Ti thermometry and U–Pb geochronology of Apollo 14 melt breccia zircons. *Contrib. Mineral. Petrol.* **169**, 30 (2015).
12. A. Nemchin, N. Timms, R. Pidgeon, T. Geisler, S. Reddy, C. Meyer, Timing of crystallization of the lunar magma ocean constrained by the oldest zircon. *Nat. Geosci.* **2**, 133–136 (2009).
13. A. A. Nemchin, R. T. Pidgeon, M. J. Whitehouse, J. P. Vaughan, C. Meyer, SIMS U–Pb study of zircon from Apollo 14 and 17 breccias: Implications for the evolution of lunar KREEP. *Geochim. Cosmochim. Acta* **72**, 668–689 (2008).

14. R. T. Pidgeon, A. A. Nemchin, W. Van Bronswijk, T. Geisler, C. Meyer, W. Compston, I. S. Williams, Complex history of a zircon aggregate from lunar breccia 73235. *Geochim. Cosmochim. Acta* **71**, 1370–1381 (2007).
15. M. Barboni, P. Boehnke, B. Keller, I. E. Kohl, B. Schoene, E. D. Young, K. D. McKeegan, Early formation of the Moon 4.51 billion years ago. *Sci. Adv.* **3**, e1602365 (2017).
16. C. A. Crow, K. D. McKeegan, D. E. Moser, Coordinated U–Pb geochronology, trace element, Ti-in-zircon thermometry and microstructural analysis of Apollo zircons. *Geochim. Cosmochim. Acta* **202**, 264–284 (2017).
17. D. Trail, M. Barboni, K. D. McKeegan, Evidence for diverse lunar melt compositions and mixing of the pre-3.9 Ga crust from zircon chemistry. *Geochim. Cosmochim. Acta* **284**, 173–195 (2020).
18. J. Greer, B. Zhang, D. Isheim, D. N. Seidman, A. Bouvier, P. R. Heck, 4.46 Ga zircons anchor chronology of lunar magma ocean. *Geochem. Perspect. Lett.* **27**, 49–53 (2023).
19. L. E. Borg, A. M. Gaffney, C. K. Shearer, A review of lunar chronology revealing a preponderance of 4.34–4.37 Ga ages. *Meteorit. Planet. Sci.* **50**, 715–732 (2015).
20. L. E. Borg, R. W. Carlson, The evolving chronology of Moon formation. *Annu. Rev. Earth Planet. Sci.* **51**, 25–52 (2023).
21. D. A. Kring, P. J. McGovern, R. W. K. Potter, G. S. Collins, M. L. Grange, A. A. Nemchin, paper presented at the *Workshop on Early Solar System Impact Bombardment III*, Houston, TX, 2015.
22. N. E. Marks, L. E. Borg, C. K. Shearer, W. S. Cassata, Geochronology of an Apollo 16 clast provides evidence for a basin-forming impact 4.3 billion years ago. *J. Geophys. Res. Planets* **124**, 2465–2481 (2019).
23. X. Chen, N. Dauphas, Z. J. Zhang, B. Schoene, M. Barboni, I. Leya, J. Zhang, D. Szymanowski, K. D. McKeegan, Methodologies for ^{176}Lu–^{176}Hf analysis of zircon grains from the Moon and beyond. *ACS Earth Space Chem.* **8**, 36–53 (2024).
24. B. Schoene, J. L. Crowley, D. J. Condon, M. D. Schmitz, S. A. Bowring, Reassessing the uranium decay constants for geochronology using ID-TIMS U–Pb data. *Geochim. Cosmochim. Acta* **70**, 426–445 (2006).
25. A. J. McKanna, B. Schoene, D. Szymanowski, Geochronological and geochemical effects of zircon chemical abrasion: Insights from single-crystal stepwise dissolution experiments. *Geochronology* **6**, 1–20 (2024).
26. J. N. Connelly, D. J. Condon, paper presented at the *Goldschmidt Conference*, Sacramento, California, 2014.
27. M. Tatsumoto, R. J. Knight, C. J. Allegre, Time differences in the formation of meteorites as determined from the ratio of lead-207 to lead-206. *Science* **180**, 1279–1283 (1973).
28. J. N. Connelly, A. A. Nemchin, R. E. Merle, J. F. Snape, M. J. Whitehouse, M. Bizzarro, Calibrating volatile loss from the Moon using the U-Pb system. *Geochim. Cosmochim. Acta* **324**, 1–16 (2022).
29. J. Hiess, D. J. Condon, N. McLean, S. R. Noble, ^{238}U/^{235}U systematics in terrestrial uranium-bearing minerals. *Science* **335**, 1610–1614 (2012).
30. B. D. Livermore, J. N. Connelly, F. Moynier, M. Bizzarro, Evaluating the robustness of a consensus ^{238}U/^{235}U value for U-Pb geochronology. *Geochim. Cosmochim. Acta* **237**, 171–183 (2018).
31. D. S. Woolum, D. S. Burnett, In-situ measurement of the rate of ^{235}U fission induced by lunar neutrons. *Earth Planet. Sci. Lett.* **21**, 153–163 (1974).
32. P. Sprung, T. Kleine, E. E. Scherer, Isotopic evidence for chondritic Lu/Hf and Sm/Nd of the Moon. *Earth Planet. Sci. Lett.* **380**, 77–87 (2013).
33. A. M. Gaffney, L. E. Borg, A young solidification age for the lunar magma ocean. *Geochim. Cosmochim. Acta* **140**, 227–240 (2014).
34. T. Iizuka, T. Yamaguchi, Y. Hibiya, Y. Amelin, Meteorite zircon constraints on the bulk Lu–Hf isotope composition and early differentiation of the Earth. *Proc. Natl. Acad. Sci. U.S.A.* **112**, 5331–5336 (2015).
35. D. J. Cherniak, W. A. Lanford, F. J. Ryerson, Lead diffusion in apatite and zircon using ion implantation and Rutherford backscattering techniques. *Geochim. Cosmochim. Acta* **55**, 1663–1673 (1991).
36. C. Meyer, I. S. Williams, W. Compston, Uranium-lead ages for lunar zircons: Evidence for a prolonged period of granophyre formation from 4.32 to 3.88 Ga. *Meteorit. Planet. Sci.* **31**, 370–387 (1996).
37. M. L. Grange, R. T. Pidgeon, A. A. Nemchin, N. E. Timms, C. Meyer, Interpreting U–Pb data from primary and secondary features in lunar zircon. *Geochim. Cosmochim. Acta* **101**, 112–132 (2013).
38. A. A. Nemchin, M. L. Grange, R. T. Pidgeon, C. Meyer, Lunar zirconology. *Aus. J. Earth Sci.* **59**, 277–290 (2012).
39. B. Zhang, Y. Lin, D. E. Moser, J. Hao, Y. Liu, J. Zhang, I. R. Barker, Q. Li, S. R. Shieh, A. Bouvier, Radiogenic Pb mobilization induced by shock metamorphism of zircons in the Apollo 72255 Civet Cat norite clast. *Geochim. Cosmochim. Acta* **302**, 175–192 (2021).
40. F. Thiessen, A. A. Nemchin, J. F. Snape, J. J. Bellucci, M. J. Whitehouse, Apollo 12 breccia 12013: Impact-induced partial Pb loss in zircon and its implications for lunar geochronology. *Geochim. Cosmochim. Acta* **230**, 94–111 (2018).
41. L. F. White, A. Černok, J. R. Darling, M. J. Whitehouse, K. H. Joy, C. Cayron, J. Dunlop, K. T. Tait, M. Anand, Evidence of extensive lunar crust formation in impact melt sheets 4,330 Myr ago. *Nat. Astron.* **4**, 974–978 (2020).
42. I. Garrick-Bethell, K. Miljković, H. Hiesinger, C. H. van der Bogert, M. Laneuville, D. L. Shuster, D. G. Korycansky, Troctolite 76535: A sample of the Moon's South Pole-Aitken basin? *Icarus* **338**, 113430 (2020).
43. J. E. Dickinson Jr., P. C. Hess, Zircon saturation in lunar basalts and granites. *Earth Planet. Sci. Lett.* **57**, 336–344 (1982).
44. S. C. Solomon, J. Longhi, Magma oceanography: 1. Thermal evolution. *Proc. Lunar Sci. Conf.* **8**, 583–599 (1977).
45. L. T. Elkins-Tanton, S. Burgess, Q.-Z. Yin, The lunar magma ocean: Reconciling the solidification process with lunar petrology and geochronology. *Earth Planet. Sci. Lett.* **304**, 326–336 (2011).
46. V. Perera, A. P. Jackson, L. T. Elkins-Tanton, E. Asphaug, Effect of reimpacting debris on the solidification of the lunar magma ocean. *J. Geophys. Res. Planets* **123**, 1168–1191 (2018).
47. M. Maurice, N. Tosi, S. Schwinger, D. Breuer, T. Kleine, A long-lived magma ocean on a young Moon. *Sci. Adv.* **6**, eaba8949 (2020).
48. M. Zhang, Y. Xu, X. Li, Effect of crustal porosity on lunar magma ocean solidification. *Acta Geochim.* **40**, 123–134 (2021).
49. A. P. Jackson, V. Perera, T. S. J. Gabriel, Impact generation of holes in the early lunar crust: Scaling relations. *J. Geophys. Res. Planets* **128**, e2022JE007498 (2023).
50. J. Meyer, L. Elkins-Tanton, J. Wisdom, Coupled thermal–orbital evolution of the early Moon. *Icarus* **208**, 1–10 (2010).
51. S. Marchi, W. F. Bottke, L. T. Elkins-Tanton, M. Bierhaus, K. Wuennemann, A. Morbidelli, D. A. Kring, Widespread mixing and burial of Earth's Hadean crust by asteroid impacts. *Nature* **511**, 578–582 (2014).
52. P. Boehnke, E. B. Watson, D. Trail, T. M. Harrison, A. K. Schmitt, Zircon saturation re-revisited. *Chem. Geol.* **351**, 324–334 (2013).
53. G. R. Osinski, E. Pierazzo, *Impact Cratering: Processes and Products* (Wiley-Blackwell, 2012).
54. R. Latypov, S. Chistyakova, R. Grieve, H. Huhma, Evidence for igneous differentiation in Sudbury Igneous Complex and impact-driven evolution of terrestrial planet proto-crusts. *Nat. Commun.* **10**, 508 (2019).
55. G. G. Kenny, J. A. Petrus, M. J. Whitehouse, J. S. Daly, B. S. Kamber, Hf isotope evidence for effective impact melt homogenisation at the Sudbury impact crater, Ontario, Canada. *Geochim. Cosmochim. Acta* **215**, 317–336 (2017).
56. J. Darling, C. Storey, C. Hawkesworth, Impact melt sheet zircons and their implications for the Hadean crust. *Geology* **37**, 927–930 (2009).
57. M. M. Wielicki, T. M. Harrison, A. K. Schmitt, Geochemical signatures and magmatic stability of terrestrial impact produced zircon. *Earth Planet. Sci. Lett.* **321**, 20–31 (2012).
58. C. I. Fassett, J. W. Head, S. J. Kadish, E. Mazarico, G. A. Neumann, D. E. Smith, M. T. Zuber, Lunar impact basins: Stratigraphy, sequence and ages from superposed impact crater populations measured from Lunar Orbiter Laser Altimeter (LOLA) data. *J. Geophys. Res. Planets* **117**, E00H06 (2012).
59. C. Orgel, G. Michael, C. I. Fassett, C. H. van der Bogert, C. Riedel, T. Kneissl, H. Hiesinger, Ancient bombardment of the inner solar system: Reinvestigation of the "fingerprints" of different impactor populations on the lunar surface. *J. Geophys. Res. Planets* **123**, 748–762 (2018).
60. P. D. Spudis, D. B. J. Bussey, S. M. Baloga, B. J. Butler, D. Carl, L. M. Carter, M. Chakraborty, R. C. Elphic, J. J. Gillis-Davis, J. N. Goswami, E. Heggy, M. Hillyard, R. Jensen, R. L. Kirk, D. LaVallee, P. McKerracher, C. D. Neish, S. Nozette, S. Nylund, M. Palsetia, W. Patterson, M. S. Robinson, R. K. Raney, R. C. Schulze, H. Sequeira, J. Skura, T. W. Thompson, B. J. Thomson, E. A. Ustinov, H. L. Winters, Initial results for the north pole of the Moon from Mini-SAR, Chandrayaan-1 mission. *Geophys. Res. Lett.* **37**, L06204 (2010).
61. G. A. Neumann, M. T. Zuber, M. A. Wieczorek, J. W. Head, D. M. H. Baker, S. C. Solomon, D. E. Smith, F. G. Lemoine, E. Mazarico, T. J. Sabaka, S. J. Goossens, H. J. Melosh, R. J. Phillips, S. W. Asmar, A. S. Konopliv, J. G. Williams, M. M. Sori, J. M. Soderblom, K. Miljković, J. C. Andrews-Hanna, F. Nimmo, W. S. Kiefer, Lunar impact basins revealed by gravity recovery and interior laboratory measurements. *Sci. Adv.* **1**, e1500852 (2015).
62. P. G. Lucey, G. J. Taylor, B. R. Hawke, P. D. Spudis, FeO and TiO_2 concentrations in the South Pole-Aitken basin: Implications for mantle composition and basin formation. *J. Geophys. Res. Planets* **103**, 3701–3708 (1998).
63. R. W. K. Potter, G. S. Collins, W. S. Kiefer, P. J. McGovern, D. A. Kring, Constraining the size of the South Pole-Aitken basin impact. *Icarus* **220**, 730–743 (2012).
64. D. M. Hurwitz, D. A. Kring, Differentiation of the South Pole–Aitken basin impact melt sheet: Implications for lunar exploration. *J. Geophys. Res. Planets* **119**, 1110–1133 (2014).
65. K. Uemoto, M. Ohtake, J. Haruyama, T. Matsunaga, S. Yamamoto, R. Nakamura, Y. Yokota, Y. Ishihara, T. Iwata, Evidence of impact melt sheet differentiation of the lunar South Pole-Aitken basin. *J. Geophys. Res. Planets* **122**, 1672–1686 (2017).
66. W. M. Vaughan, J. W. Head, Impact melt differentiation in the South Pole-Aitken basin: Some observations and speculations. *Planet. Space Sci.* **91**, 101–106 (2014).
67. M. J. Jones, A. J. Evans, B. C. Johnson, M. B. Weller, J. C. Andrews-Hanna, S. M. Tikoo, J. T. Keane, A South Pole–Aitken impact origin of the lunar compositional asymmetry. *Sci. Adv.* **8**, eabm8475 (2022).

68. F. J. Stadermann, E. Heusser, E. K. Jessberger, S. Lingner, D. Stöffler, The case for a younger Imbrium basin: New ^{40}Ar-^{39}Ar ages of Apollo 14 rocks. *Geochim. Cosmochim. Acta* **55**, 2339–2349 (1991).
69. C. H. Simonds, J. L. Warner, P. E. McGee, A. Cochran, R. W. Brown, paper presented at the *Conference on Luna 24*, Houston, TX, 1977.
70. R. E. Merle, A. A. Nemchin, M. J. Whitehouse, R. T. Pidgeon, M. L. Grange, J. F. Snape, F. Thiessen, Origin and transportation history of lunar breccia 14311. *Meteorit. Planet. Sci.* **52**, 842–858 (2017).
71. J. J. Papike, S. B. Simon, J. C. Laul, The lunar regolith: Chemistry, mineralogy, and petrology. *Rev. Geophys.* **20**, 761–826 (1982).
72. T. C. Labotka, M. J. Kempa, C. White, J. J. Papike, J. C. Laul, The lunar regolith: Comparative petrology of the Apollo sites. *Proc. Lunar Sci. Conf.* **11**, 1285–1305 (1980).
73. G. B. Dalrymple, G. Ryder, Argon-40/argon-39 age spectra of Apollo 17 highlands breccia samples by laser step heating and the age of the Serenitatis basin. *J. Geophys. Res. Planets* **101**, 26069–26084 (1996).
74. D. P. Blanchard, L. A. Haskin, J. W. Jacobs, J. C. Brannon, R. L. Korotev, Major and trace element chemistry of Boulder 1 at Station 2, Apollo 17. *The Moon* **14**, 359–371 (1975).
75. C.-Y. Shih, L. E. Nyquist, B. M. Bansal, H. Wiesmann, Rb-Sr and Sm-Nd chronology of an Apollo 17 KREEP basalt. *Earth Planet. Sci. Lett.* **108**, 203–215 (1992).
76. J. M. Mattinson, Zircon U–Pb chemical abrasion ("CA-TIMS") method: Combined annealing and multi-step partial dissolution analysis for improved precision and accuracy of zircon ages. *Chem. Geol.* **220**, 47–66 (2005).
77. D. J. Condon, B. Schoene, N. M. McLean, S. A. Bowring, R. R. Parrish, Metrology and traceability of U–Pb isotope dilution geochronology (EARTHTIME Tracer Calibration Part I). *Geochim. Cosmochim. Acta* **164**, 464–480 (2015).
78. N. M. McLean, D. J. Condon, B. Schoene, S. A. Bowring, Evaluating uncertainties in the calibration of isotopic reference materials and multi-element isotopic tracers (EARTHTIME Tracer Calibration Part II). *Geochim. Cosmochim. Acta* **164**, 481–501 (2015).
79. T. E. Krogh, A low-contamination method for hydrothermal decomposition of zircon and extraction of U and Pb for isotopic age determinations. *Geochim. Cosmochim. Acta* **37**, 485–494 (1973).
80. H. Gerstenberger, G. Haase, A highly effective emitter substance for mass spectrometric Pb isotope ratio determinations. *Chem. Geol.* **136**, 309–312 (1997).
81. D. Szymanowski, B. Schoene, U-Pb ID-TIMS geochronology using ATONA amplifiers. *J. Anal. At. Spectrom.* **35**, 1207–1216 (2020).
82. J. F. Bowring, N. M. McLean, S. A. Bowring, Engineering cyber infrastructure for U-Pb geochronology: Tripoli and U-Pb_Redux. *Geochem. Geophys. Geosyst.* **12**, Q0AA19 (2011).
83. N. M. McLean, J. F. Bowring, S. A. Bowring, An algorithm for U-Pb isotope dilution data reduction and uncertainty propagation. *Geochem. Geophys. Geosyst.* **12**, Q0AA18 (2011).
84. A. H. Jaffey, K. F. Flynn, L. E. Glendenin, W. C. Bentley, A. M. Essling, Precision measurement of half-lives and specific activities of ^{235}U and ^{238}U. *Phys. Rev. C* **4**, 1889–1906 (1971).
85. U. Schärer, The effect of initial ^{230}Th disequilibrium on young U-Pb ages: The Makalu case, Himalaya. *Earth Planet. Sci. Lett.* **67**, 191–204 (1984).
86. B. Schoene, M. P. Eddy, K. M. Samperton, C. B. Keller, G. Keller, T. Adatte, S. F. R. Khadri, U-Pb constraints on pulsed eruption of the Deccan Traps across the end-Cretaceous mass extinction. *Science* **363**, 862–866 (2019).
87. A. J. McKanna, I. Koran, B. Schoene, R. A. Ketcham, Chemical abrasion: The mechanics of zircon dissolution. *Geochronology* **5**, 127–151 (2023).
88. B. Schoene, C. Latkoczy, U. Schaltegger, D. Günther, A new method integrating high-precision U–Pb geochronology with zircon trace element analysis (U–Pb TIMS-TEA). *Geochim. Cosmochim. Acta* **74**, 7144–7159 (2010).
89. L. O'Connor, D. Szymanowski, M. P. Eddy, K. M. Samperton, B. Schoene, A red bole zircon record of cryptic silicic volcanism in the Deccan Traps India. *Geology* **50**, 460–464 (2022).
90. D. Trail, N. Tailby, Y. Wang, T. Mark Harrison, P. Boehnke, Aluminum in zircon as evidence for peraluminous and metaluminous melts from the Hadean to present. *Geochem. Geophys. Geosyst.* **18**, 1580–1593 (2017).

Acknowledgments: We thank CAPTEM (Curation and Analysis Planning Team for Extraterrestrial Materials) and the Lunar Sample curators at the Johnson Space Center who made samples available for this research. Thanks also to J. Hanchar for providing the synthetic MUNZirc zircon reference materials. **Funding:** This work was supported by NASA Emerging Worlds Program grant NNH18ZDA001N-EW (to K.D.M., M.B., B.S., and N.D.) and NSF grants EAR-1726099 and EAR-1735512 (to B.S.). The UCLA ion microprobe laboratory is partially supported by a grant from the NSF Instrument and Facilities Program. **Author contributions:** Conceptualization: M.B., K.D.M., and B.S. Methodology: D.S., B.S., M.B., X.C., Z.J.Z., and N.D. Investigation: M.B., D.S., B.S., X.C., Z.J.Z., and N.D. Visualization: D.S., M.B., and B.S. Writing–original draft: M.B., D.S., B.S., and K.D.M. Writing–review and editing: M.B., D.S., B.S., N.D., Z.J.Z., and K.D.M. Funding acquisition: K.D.M., M.B., B.S., and N.D. **Competing interests:** The authors declare that they have no competing interests. **Data and materials availability:** All data needed to evaluate the conclusions in the paper are present in the paper and/or the Supplementary Materials.

Submitted 10 January 2024
Accepted 21 June 2024
Published 24 July 2024
10.1126/sciadv.adn9871